Leachability of rare-earth, calcium and minor metal ions from natural Fluorapatite in perchloric, hydrochloric, nitric and phosphoric acid solutions: Effect of proton activity and anion participation

Bandara, A.M.T.S.; Senanayake, G.

Leachability of rare-earth, calcium and minor metal ions from natural fluoroapatite in perchloric, hydrochloric, nitric and phosphoric acid solutions : Effect of proton activity and anion participation

A.M.T.S. Bandara, G. Senanayake*
Chemical & Metallurgical Engineering & Chemistry, School of Engineering & Information Technology, Murdoch University, 90 South Street, Murdoch, Perth WA6150, Australia

Abstract

Highly technological applications of rare earth (RE) metals and scarcity of supply have become an incentive to recover the REs from various resources, which include high grade and low grade ores, as well as recycled waste materials. The co-existence of RE and non-RE minerals and their different reactivities with acids affect the leaching behavior of metal ions highlighting the importance of detailed studies using dfferent types of ores/concentrates in different acids to compare and contrast the leaching behaviour of RE and non-RE metal ions. A natural fluoroapatite (FAP) sample from Harts Range, Northern Territory, Australia was assayed and characterised using standard techniques which indicated the presence of 33.8% Ca, 12.6% P, 0.32% Sr, 0.22% Fe, 0.19% Na, 0.09% Si and 0.01-0.24% RE (0.24% Ce, 0.11% La, 0.10% Nd, 0.03% Pr, 0.02% Sm, 0.02% Gd, 0.02% Y, 0.01% Dy). The XRD patterns identified the presence of FAP ($Ca_5(PO_4)_3F$), carbonate-FAP ($(Ca_5(PO_4,CO_3)_3F$), calcite ($CaCO_3$) and traces of some RE minerals, namely cheralite ($(Ca,Ce)(Th,Ce)(PO_4)_2$), monazite ($(Ce,La,Th,Nd,Y)PO_4$), britholite ($(Na,Ce,Ca)_5(OH,F)((P,Si)O_4)_3$) and kainosite ($Ca_2(Ce,Y)_2(SiO_4)_3CO_3.H_2O$). It is possible that the FAP contains part of the RE within the lattice and the balance as ultrafine inclusions of RE minerals which affect the leaching behaviour of RE incorporated in FAP. The leaching in perchloric, hydrochloric, nitric, and phosphoric acid solutions (2.28 or 3.25 mol/L) at 95^{o}C was conducted using particles of size range 150-180 µm, 5% (w/w) solids and a stirring rate of 1100 rpm. The similarities and differences in leaching efficiencies of metal ions are rationalised on the basis of proton activity of acids and the participation of anions due to complexation with metal ions. The leaching efficiency of calcium, phosphate, fluoride, sodium and strontium reached 80-100% after 5-10 min in hydrochloric, perchloric and nitric acid compared to lower leaching efficiencies (<40%) in phosphoric acid. Despite the low solubility products of phosphates of iron(III) and calcium ($pK_{SP} \approx 24, 31$), the higher pH, and lower proton activity of phosphoric acid, the higher leaching efficiencies of calcium and iron (≥80%) suggest the formation of complex species of these metal ions with phosphate ions. The leaching efficiencies of lanthanum, cerium and neodymium were low in all acids and showed a descending order: $HClO_4$ (54-63%) > HCl (21-13%) > HNO_3 (5-7%). The RE leaching efficiency in $HClO_4$ remained relatively unaffected with time, but the low leaching efficiencies in other acids after 30 min (<20%) indicates the precipitation of RE-phosphates and prospect of selective leaching of FAP. The slope of linear correlation of leaching efficiency of REs was close to unity in $HClO_4$, HCl and HNO_3 indicating similar behaviour. A higher slope for La-Ce leaching efficiency correlation of 1.8 compared to 0.9 for Nd-Ce in H_3PO_4 warrants further studies.

Keywords: Rare earth metals, Natural fluorapatite, Leaching efficiency, Proton activity, Anion participation

*Tel.: +61 8 93602833; fax: +61 8 93606343.
E-mail address: G.Senanayake@murdoch.edu.au

1. Introduction

The elements in the lanthanide series, yttrium and scandium are considered as rare earth (RE) elements and they have similar chemical properties. Most of the RE deposits exist in China, America, India, Middle Asian nations, South Africa, Australia, and Canada (Zhang and Edwards, 2012). Global RE reserves and the production of oxides are listed in Table 1. The demand for REs has increased in recent years due to uncertainty of the supply and the high technological applications associated with their characteristic electronic, optical and magnetic properties (Gupta and Krishnamurthy, 2005). The estimated global demand of RE oxides is 0.125 Mt (2013), 0.136 Mt (2014), 0.148 Mt (2015) and 0.160 Mt (2016) (IMCOA, 2013). Thus, interest in the recovery of REs from low grade ores, clays, slags, and secondary sources such as spent batteries and electronic waste has also gathered momentum due to increasing demand and scarcity as well as the need for reducing environmental pollution caused by the discarded waste (Fernandes et al., 2013; Jordens et al., 2013; Kim and Osseo-Asare, 2012; Kim et al., 2014; Kul et al., 2008; Kuzmin et al., 2012; Li et al., 2009; Lister et al., 2014; Moldoveanu et al., 2012, 2013; Panda et al., 2014; Resende and Morais, 2010; Tunsu et al., 2014; Wang et al., 2010).

The RE phosphate minerals (Table 2) are the most naturally abundant forms that are associated with fluorapatite (FAP) of chemical formula $Ca_5(PO_4)_3F$. The RE site occupancies in the FAP lattice structure are normally via the two calcium atoms, having different stereochemistry in the atomic arrangement of FAP as denoted by Ca1 and Ca2 in Fig. 1 (Fleet and Pan, 1995). While Ca1 is surrounded by nine oxygen atoms, forming a tricapped trigonal prism, Ca2 is surrounded by six oxygen atoms and one fluorine atom, forming an irregular polyhedron. These RE site occupancies are generally consistent with site preferences, deduced from bond-valence calculations, which show that the substitutions for calcium lead to an

equalisation of Ca1 and Ca2 bond valences. Moreover, the RE site occupancy ratio correlates inversely with fluoride bond valence (Fleet and Pan, 1995). As a result, FAP is considered as a RE concentrating mineral and its chemical formula becomes $(Ca,RE..)_5(PO_4)_3F$ (Table 2). The RE content in FAP as RE-oxides varies from trace amounts to over 10% and the RE content in phosphate sources as RE-oxides has been estimated at over 8 million metric tons (Gupta and Krishnamurthy, 2005). In addition to REs, sodium can also be associated with FAP, resulting in the chemical formula $(Na,Ca)_5(PO_4)_3F$ (Chakhmouradian et al., 2002; McClellan and Lehr, 1969). Britholite is a sub group of FAP and its mineralogy (Table 2) shows the association of sodium in phosphate minerals. The association of strontium with calcium and carbonate with phosphate form $(Ca,Sr)_5(PO_4)_3F$ and $Ca_5(PO_4,CO_3)_3F$, respectively, where the latter is considered as carbonate-fluoroapatite (Chakhmouradian et al., 2002; McClellan and Lehr, 1969)

Depending upon the mineralogy, gravity-flotation, magnetic-flotation, and desliming-flotation have been the most commonly used techniques for concentrating RE minerals prior to extraction of REs (Zhang and Edwards, 2012). A pre-leach stage with mineral acids (Eqs. 1-5) can be useful in order to selectively leach the FAP fraction as well as other impurities such as sodium, potassium, magnesium, aluminum, iron, manganese, uranium, and thorium associated with the FAP lattice (Table 2), resulting in a RE enriched concentrate for further processing. However, leaching efficiencies can vary significantly depending upon the mineralogy of the ore and the type of acid used. Although the intention is for selective leaching of FAP, any REs along with other metal ions associated with the FAP lattice (Fig. 1) are also likely to leach. Moreover, the H_3PO_4 and HF formed during the leaching process of FAP with other acids (Eqs. 1-5) can interfere and change the leaching efficiency of FAP and other metal ions (REs and non-REs)

through complexation with phosphate and fluoride ions, or precipitation as phosphate or other salts.

$$Ca_5(PO_4)_3F + 10HCl = 5CaCl_2 + 3H_3PO_4 + HF \quad (1)$$

$$Ca_5(PO_4)_3F + 10HNO_3 = 5Ca(NO_3)_2 + 3H_3PO_4 + HF \quad (2)$$

$$Ca_5(PO_4)_3F + 10HClO_4 = 5Ca(ClO_4)_2 + 3H_3PO_4 + HF \quad (3)$$

$$Ca_5(PO_4)_3F + 7H_3PO_4 = 5Ca(H_2PO_4)_2 + HF \quad (4)$$

$$Ca_5(PO_4)_3F + 5H_2SO_4 + 5xH_2O = 5CaSO_4.xH_2O + 3H_3PO_4 + HF \quad (x = 2 \text{ or } 0.5) \quad (5)$$

Complex mineralogy due to the co-existence of RE and non-RE minerals and their reactivity with different lixiviants affect the leaching behavior of metal ions from low grade and high grade ores. This highlights the importance of detailed studies using both types of ores/concentrates. Despite the difficulty of the mineralogical identification of RE minerals associated with FAP, due to low grades, the direct leaching of FAP in different acids can shed light on the dissolution behavior of RE and other metal ions associated with FAP. This work aims to briefly review the relevant literature and investigate the effect of $HClO_4$, HCl, HNO_3 and H_3PO_4 on the leaching behavior of non-RE elements (Ca, P, F, Na, Sr, Fe) and RE elements (La, Ce and Nd) from a natural FAP sample at 95 ^oC. The high temperature of 95 ^oC was chosen to facilitate selective leaching of FAP by minimizing the dissolution of RE and maximizing the dissolution of FAP based on the previous studies by Wang et al. (2010) and Olanipekun (1999), respectively. The main aim is to understand the various interactions between cations and anions involved in the multi cation-anion system formed during the leaching of FAP with low RE content which allows the extension of this comparative investigation to RE rich phosphate ores/concentrates.

2. Previous studies

The FAP leaching in different acid systems such as H_3PO_4, HCl, H_2SO_4 and various mixtures of acids/salts has been extensively studied (Table 3). The main focus has been the investigation of thermodynamics and kinetics of FAP dissolution and the effect of pH, temperature and concentration/composition of the lixiviant. Sluis et al. (1987) reported that the rate of leaching of FAP is controlled by the diffusion of calcium ions. Brahim et al. (2008) also concluded that the dissolution of synthetic FAP in H_3PO_4 obeys a diffusion controlled reaction at temperatures below 45 ^oC while it is a chemically controlled process at higher temperatures. Antar and Jemal (2008) noted that in a mixture of H_3PO_4 and H_2SO_4 there are three reaction domains, namely, the dissolution of FAP and neutralization of $H_2PO_4^-$, the precipitation of gypsum in the form of hemihydrate ($CaSO_4.0.5H_2O$), and the transformation of hemihydrate to dihydrate ($CaSO_4.2H_2O$). Elevated temperatures and the addition of HCl enhance the dissolution of FAP in H_2SO_4 (Olanipekun, 1999). A general rate equation has been derived for FAP dissolution in a range of temperatures and pH used in the experiment (Chaïrat et al., 2007). Likewise, the logarithmic values of initial dissolution rates showed a linear dependence on pH of the solution (Harouiya et al., 2007). The use of 9.6% (w/w) citric acid caused the leaching of 98–100% of fluoride from FAP with low leaching efficiencies of aluminium and iron (Al-Othman and Sweileh, 2000). The leaching behavior of REs which can be present in FAP in trace amounts has not been discussed in any of the studies summarised in Table 3. This highlights the need for a systematic study in order to rationalise the leaching behaviour of cations and anions associated with natural FAP in different types of acids, which can be extended to other feed materials.

Selective leaching of REs from FAP is unsuccessful with sulphuric acid as calcium tends to precipitate as hemihydrates or dihydrates. Only 20-30% leaching of REs and yttrium can be achieved from phosphate minerals with sulphuric acid in the presence of FAP (Wang et al., 2010). In contrast, more than 98% leaching efficiency of REs, along with yttrium, from both low grade and high grade xenotime concentrates with no FAP has been achieved after digestion with 98% sulphuric acid at 250^{o}C and solid/liquid ratio of 1.0/2.5 for 6 h followed by water leaching (Vijayalakshmi et al., 2001). The conversion of RE phosphates to RE sulphates during this acid digestion facilitate the water leaching of RE. It has been reported that the leaching efficiency of neodymium from an apatite ore is about 40% with 4 mol/L HNO_3, compared to 7% with 2 mol/L H_2SO_4 acid (Preston et al., 1996). This difference is also a result of the precipitation of gypsum with sulphuric acid. In contrast, the precipitation of rare earth double sulphate salts, $NaRE(SO_4)_2$, occurs in sulphuric acid solutions in the presence of sodium ions (Senanayake et al., 2014a). These issues highlight the advantages of the selective leaching of FAP fraction in a pre-leach stage.

3. Experimental

3.1 *Characterisation of fluorapatite*

A bulk fluorapatite sample from Harts Range, Northern Territory, Australia was subjected to crushing in a pulverising ring mill, homogenising and screening. Further grinding and sieving produced a sample of FAP of particle size range 150 – 180 µm. The ground material was quantitatively assayed using inductively coupled plasma – atomic emission spectroscopy (ICP-AES) / mass spectroscopy (ICP-MS) and X-Ray Fluorescence (XRF) analysis. Moreover, the feed material was analysed using X-Ray Diffractometer (GBC Enhanced Mini-material Analyser (EMMA), Theta-Theta Difractometer), Scanning electron microscopy/Energy

Dispersive Spectroscopy (JSM – 6000), Fourier-transform infrared spectroscopy, and Raman spectroscopy (Nicolet 6700 FT-IR spectrometer equipped with NXR FT-Raman module).

3.2 Leaching studies

The leaching experiments were conducted at 5% (w/w) solids using a reactor described in previous publications (Senanayake et al., 2010) with 800 mL of each acid at the desired concentrations and a rotation speed of the agitator maintained at 1100 rpm for all experiments. The liquor samples, withdrawn through 0.22 µm filters at different time intervals during a period of 30 minutes, or 4 hours in the case of phosphoric acid, were quantitatively analysed using ICP-AES/MS technique at the TSW laboratories in Perth, Western Australia. Fluoride analysis of the leach liquors was conducted using a commercial fluoride combination electrode (Orion, Model 9609BNWP) in conjunction with a Thermo Scientific Orion Star A214 Benchtop pH/ISE meter. The pH values were measured using a commercial double junction pH electrode (TPS 121207) in conjunction with an Aqua-pH Waterproof pH-mV Temperature meter.

4. Results and discussion

4.1 Characterisation of feed material

4.1.1 ICP – AES/MS analysis

The results listed in Table 4 show that the mass percentages of Ca (33.8%) and P (12.6%) are very high compared to that of total rare earths (TREs), ~0.55%, and other minor elements in the range of 0.01% - 0.32% in FAP. The theoretical Ca/P molar ratio of pure FAP is 1.7/1.0. However, the results listed in Table 4 correspond to a Ca/P molar ratio of 2.1/1.0. This suggests the possibility of the presence of carbonate-FAP ($Ca_5(PO_4,CO_3)_3F$) and calcite ($CaCO_3$). The assays also show the presence of Na, Sr, Fe and REs (La, Ce and Nd are major) in FAP and

hence, a trace amount of FAP associated with these elements, or the presence of other minerals containing these elements described in Table 2.

4.1.2 XRD, SEM and EDS analysis

The presence of FAP, carbonate-FAP, calcite and a trace amount of some RE minerals, namely cheralite, monazite, britholite and kainosite (RE silicate and carbonate, Table 2), can be identified by XRD patterns shown in Fig. 2. As shown in Table 4, REs are present in small quantities and therefore, the corresponding peaks have very low relative intensities in Fig. 2. The SEM image and Energy Dispersive Spectroscopy (EDS) of FAP are shown in Fig. 3a-b. The elemental analysis based on EDS indicates the mass percentages of 32.1% Ca, 15.1% P and 0.74% F. These percentages of calcium and phosphorous correspond to a molar ratio of Ca/P = 1.65/1.0 which is closer to the expected ratio of 1.7/1.0 for FAP, but is lower than the molar ratio of Ca/P = 2.1/1.0 determined by ICP-AES/MS analysis of FAP listed in Table 4.

4.1.3 FT-IR and Raman spectroscopy

Figs. 4 and 5 represent the FT-IR and Raman spectra of FAP, respectively. The assigned bands of these spectra are listed in Tables 5 and 6. All four vibrational modes of PO_4^{3-} denoted by $\nu_1(a_1)$, ν_2(e), $\nu_3(f_2)$ and $\nu_4(f_2)$ are Raman active while $\nu_3(f_2)$ and $\nu_4(f_2)$ are only IR active. All vibrational modes of CO_3^{2-} are both IR and Raman active except $\nu_1(a^1{}_1)$ and $\nu_2(a^{11}{}_2)$ where $\nu_1(a^1{}_1)$ is IR inactive whilst $\nu_2(a^{11}{}_2)$ is Raman inactive. Nevertheless, all vibrational modes of SiO_2 are both Raman and IR active. This spectroscopic analysis shows the presence of calcite in the feed materials as bands can be assigned for CO_3^{2-} ions. As the amount of silica present (0.09%) is very low, bands cannot be assigned for it.

4.2 Leaching of calcium, phosphate and fluoride

4.2.1 Leaching results

Table 7 shows that 100% leaching efficiency of calcium, phosphate and fluoride can be achieved after 30 min using 3.25 mol/L acids (HCl, HNO_3 and H_3PO_4). Fig. 6a shows the leaching pattern of calcium within the first 30 minutes of the 4 h leaching duration in all four acids. The complete leaching of calcium occurred within the 1st minute, soon after the leaching process started in 1.30 mol/L HCl, HNO_3 and $HClO_4$. The 1:1 leaching of Ca and P in all three acids after 1 minute is also evident (Fig. 6b). Fig. 6a also shows the leaching kinetics of calcium during the first 30 min and highlights the initial relative rates in different acids which follow the descending order: HNO_3 > HCl > $HClO_4$ > H_3PO_4. These results indicate the effect of free acid (H^+) concentration and/or the beneficial effect of the anions NO_3^- and Cl^- compared to $H_2PO_4^-$ and warrant further discussion.

4.2.2 Relative effects of acids

Unlike the three strong mono-protic acids HCl, HNO_3 and $HClO_4$ which are completely dissociated in water, H_3PO_4 and HF formed according to Eqs. (1)-(5) are weak acids. It is important to consider the partial dissociation of H_3PO_4 and HF in equations (1)-(5), protonated and un-protonated soluble species of phosphate and fluoride, as well as other reactions which involve interactions between metal ions and ligands which influence solubility and leaching kinetics (Senanayake, 2007; Senanayake et al., 2014b). Chemical equations for dissociation of H_3PO_4 and HF produced in equations (1)-(5), and CO_2 produced by the leaching of carbonate associated with FAP (only small quantities) as well as other reactions are shown by equations (6)-(24) in Table 8, along with their equilibrium constants. The species HA in Eq. (25) is

considered as a weak acid. For the dissociation of HA, the concentration ratio $[A^-]/[HA]$ is related to the equilibrium constant (K_H or K_a) and pH according to Equation (26) where $pK_H = -\log K_H$. According to this relationship when the pH of the solution is equal to pK_H, the two species HA and A^- in solution exist in equimolar concentrations (50% each). The species A^- predominates in solutions of pH greater than pK_H (i.e. $[A^-] > 50\%$, $[HA] < 50\%$).

$$HA = H^+ + A^- \quad \text{(Equilibrium constant} = K_a \text{ or } K_H) \tag{25}$$

$$pH = pK_H + \log[A^-]/[HA], \text{ where } pK_H = pK_a = -\log K_a \tag{26}$$

$$pF = pK_F + \log\{[HF]/[HF_2^-]\}, \text{ where } pK_F = -\log K_F \tag{27}$$

$$\%\ \text{of}\ A^- = 100\left(\frac{10^{(pH-pK)}}{1 + 10^{(pH-pK)}}\right), \text{where } pK = pK_a = pK_H \tag{28}$$

Based on the pK_H values from the HSC 7.1 database (Roine, 2012), Fig.7a-b shows the effect of temperature on pK_H which in turn shows the predominant regions of protonated (HA) and unprotonated (A^-) species relevant to the reactions in Equations (6)-(12) listed in Table 8. The change in temperature does not seem to have a significant influence on pK_H values. In a solution of a given concentration of phosphorus(V) at pH values below line (i) in Fig. 7a (read pH from y-axis), the predominant form of phosphorus(V) is the neutral species $H_3PO_4^0$, whilst the anion $H_2PO_4^-$ predominates at pH values above line (i). The dinegative anion HPO_4^{2-} predominates at pH values above line (ii) in Fig. 7a. The same principle applies to the reaction in Eq. (8) and line (iii). Likewise, Fig. 7b shows the predominant regions of pH in the two cases of $HF_2^-/HF^0/F^-$ indicated by lines (iv)/(v) and $CO_2/HCO_3^-/CO_3^{2-}$ shown by lines (vi)/(vii).

Fig. 8 plots the effect of acid concentration on the measured pH and proton activity (a_{H^+}) of HCl and $HClO_4$ (Majima and Awakura, 1981; Senanayake, 2007). The measured value of pH using a glass-calomel combined electrode, after correcting for liquid junction potentials, represent a_{H^+} (pH = -log a_{H^+}) which can be expressed as the ratio $[H(H_2O)_h^+]/(a_w)^h$ where $[H(H_2O]_h^+]$ is the concentration of H^+ in solution, a_w is the activity of water, and h is the hydration number of H^+. Thus, the increase in H^+ activity with the increase in concentration in Fig. 8 is a result of the increase in $[H(H_2O)_h^+]$ and the decrease in a_w (Senanayake, 2007). The water activity and thus proton activity of a given acid solution are expected to change with changes in temperature. Nevertheless, the measured activities at 25 ^oC have been used to interpret the kinetics and reaction mechanisms of leaching of oxides and sulphides in comparative studies (Majima and Awakura, 1981; Senanayake and Muir, 2003; Senanayake, 2007). At the measured pH of ~1 of 3.25 mol/L H_3PO_4 at 25 ^oC (this work), the stable species in solution, according to Fig. 7a-b, are H_3PO_4 and HF. According to Fig. 8 the measured activity of H^+ at 3.25 mol/L acid follows the order $HClO_4$ > HCl > H_3PO_4 and suggests that the lower rate of calcium leaching in H_3PO_4 is largely due to the lower activity of H^+.

The possible effect of the complexation of anions such as chloride can be examined by comparing the association constants of the dissolving cation with the anion (Senanayake, 2007). The descending order of the formation constants at 25 ^oC (shown in brackets) for different ion-associates between Ca^{2+} and anions is: $CaHPO_4^0$ ($10^{2.8}$) > CaF^+ ($10^{0.68}$) > $CaCl^+$ ($10^{0.15}$) > $CaCl_2^0$ ($10^{-0.64}$) (HSC 7.1 data base and Table 8), whereas the association of perchlorate ion with cations is generally considered to be much weaker. The comparison of the activity of H^+, anion-association constant of Ca^{2+} and the leaching kinetics of calcium from FAP can be used to rationalise the relative rates. Despite the higher association constants of $CaHPO_4^0$ the leaching

rate of Ca^{2+} in H_3PO_4 is lower due to lower H^+ activity. Likewise, despite the lower activity of H^+ in HCl compared to that of $HClO_4$, the leaching rate of Ca^{2+} in HCl is higher due to the influence of Cl^- caused by ion-association with Ca^{2+}.

4.2.3 Diffusion controlled reaction

Fig. 9 examines the applicability of shrinking sphere/core kinetic models for the initial dissolution of calcium ions from FAP in 3.25 mol/L H_3PO_4 according to Eqs. (29) and (30), respectively, and the general expression A(a) + bB(s) → products, where X is the fraction dissolved after time t (s), k_{ap} = apparent rate constant (s^{-1}), b = stoichiometric factor, c = concentration of reactant (mol cm^{-3}), ρ = molar density (mol cm^{-3}) of the dissolving metal in the particle, d_o (cm) = initial particle diameter, k_i = intrinsic rate constant of the surface reaction (cm s^{-1}), D = diffusivity (cm^2 s^{-1}) of the species through a product layer, ε = particle porosity.

$$1-(1-X)^{1/3}=\left(\frac{2bk_ic}{\rho d_o}\right)t=k_{ap}t \tag{29}$$

$$1-3(1-X)^{2/3}+2(1-X)=\left(\frac{6bDc}{(1-\varepsilon)\rho d_o^2}\right)t=k_{ap}t \tag{30}$$

According to these models, the chemical reaction at the particle surface (Eq. (29)) or the diffusion of reactants or products through a thickening product layer around the particle (Eq. (30)) is rate controlling (Levenspiel, 1972). The linear relationship in Fig. 9 based on Eq. 30 shows a better correlation than that based on Eq. (29). However, despite the applicability of Eq. (30) for initial leaching, complete dissolution is achieved at latter stages (after 10 min, Fig. 6a) indicating the removal of the surface blocking product layer. In contrast, if the acid strength is lowered from 3.25 to 2.28 mol/L H_3PO_4, the leaching of calcium from FAP decreases to 75%,

respectively, whilst fluoride leaching remains at 100% (Table 7). As noted in section 4.1.2 the molar ratio of Ca/P of FAP based on EDS is 1.65/1.0, which is closer to the expected value of 1.7/1.0 for FAP. However, the higher leaching efficiency of fluoride (100%) compared to that of calcium (75%) in 2.28 mol/L H_3PO_4 (Table 7) indicates that the surface is changing from the FAP structure in Fig. 1 to a calcium rich product layer and warrants further investigation, which is beyond the scope of this work.

4.3 Leaching of minor elements and RE

4.3.1 Na, Fe and Sr

The mass percentages (Table 4) of sodium (0.19%), iron (0.22%) and strontium (0.32%) in the FAP sample are very small compared to that of calcium (33.8%). However, the leaching behavior of sodium and strontium is generally similar to calcium, as described previously. As shown in Table 7 and Fig. 10, sodium and strontium show high leaching efficiency (≥80%) in the three acids HCl, $HClO_4$ and HNO_3 after 10 min with 100% leaching efficiency of sodium observed in HCl, HNO_3 and $HClO_4$ after 10-30 min. In comparison, the limited leaching efficiency of 80% sodium and iron in H_3PO_4 is a result of the low proton activity as well as the presence of silicates.

Unlike calcium, strontium shows a low leaching efficiency in H_3PO_4 (Fig. 10d), compared to higher leaching efficiencies in other acids, indicating the formation of complex species such as $CaHPO_4^0$ and $Ca(H_2PO_4)^+$ with large equilibrium constants listed in Table 8. Such information on the complexes of strontium for the purpose of comparison is lacking. Likewise, the leaching efficiency of iron is sensitive to the type of acid where the leaching efficiency after 10 min follows the descending order: H_3PO_4 (74%) > $HClO_4$ (45%) > HCl (28%)

> HNO_3 (26%). This trend demonstrates the role of higher proton activity in $HClO_4$ compared to that in HCl (Fig. 8a). Although the higher pH and lower H^+ activity in H_3PO_4 is generally detrimental for leaching, the formation of iron(III) complexes such as $Fe(H_2PO_4)^{2+}$, $FeF_n^{(3-n)+}$ where (n = 1, 2, 3, 4) as shown in Table 8 appears beneficial for iron leaching.

4.3.2 La, Ce and Nd

Despite the low composition of RE in the FAP sample (0.10-0.24% La, Ce and Nd), the leaching behaviour is sensitive to the type of acid. As shown in Table 7 and Fig. 11, high leaching efficiencies are observed in $HClO_4$. One of the key differences in the leaching behaviour of RE from other minor elements described in section 4.3.1 is the generally low leaching efficiency in all four acids and the descending order: $HClO_4$ (54-63%) > HCl (21-13%) > HNO_3 (5-7%) shown in Fig. 10a,b,c. In the case of H_3PO_4 the general trend is that highest leaching efficiencies are shown after 10 min in the descending order: La (59%) > Ce (38%) > Nd (26%). It is possible that the FAP contains part of the RE within the lattice and the balance as ultrafine inclusions of RE minerals which affect the leaching behaviour of RE incorporated in FAP. All REs appear to precipitate during prolonged leaching after 10 min, in the cases of hydrochloric and phosphoric acid (Fig. 10-11). Higher leaching efficiencies of RE in $HClO_4$ in Fig. 10c is consistent with that of calcium, whilst the very low leaching efficiencies in HNO_3 can be related to the oxidising ability of HNO_3, which may precipitate Ce(IV) compounds.

The behaviour of all three REs in $HClO_4$ is similar as in HNO_3, although the leaching in $HClO_4$ is higher than that in HNO_3. Fig. 12 shows a good linear correlation of slope close to unity for the leaching efficiencies of lanthanum and neodymium as a function of that of cerium

in $HClO_4$ and HCl, indicating that the anions ClO_4^- and Cl^- have no significant effect on the dissolution of REs. However, in the case of H_3PO_4, as shown in Fig. 12b, a higher slope of 1.8 for lanthanum compared to 0.9 for neodymium indicates the sensitivity of the RE bearing minerals to acidity and/or the relative interactions of RE cations with anions such as $H_2PO_4^-$ and F^-. The stability constants and pK_{sp} values listed in Table 9 are too close for comparison of the three REs but the stability of $RE(H_2PO_4)^{2+}$ follows the descending order La > Ce >Nd. This may explain the different slopes in Figs. 12a-b but warrants further studies. Despite the 20-60% leaching in phosphoric acid after 10 min, which remained relatively unaffected with time, the lower leaching efficiencies in other acids after 30 min (<20%) indicates the precipitation of RE-phosphates which facilitates selective leaching of FAP.

4. Conclusions

A comparative leaching study of natural fluoroapatite of low RE content in $HClO_4$, HNO_3, HCl, and H_3PO_4 provides useful information on the behaviour of major/minor elements as well as REs leading to several conclusions. The leaching of calcium, sodium, and strontium is facilitated by high proton activity in $HClO_4$ compared to low proton activity in H_3PO_4, but 80-100% leaching occurs after 10-30 mins. Anions such as chloride, phosphate and fluoride show beneficial effects indicating the association of anions with calcium, and iron cations. The leaching efficiency of REs is also sensitive to proton activity as evident from the descending order: $HClO_4$ (54-63%) >HCl (13-21%) > HNO_3 (5-7%) after 30 min, where the precipitation of Ce(IV) compounds due to the oxidising ability of HNO_3, is likely to cause very low RE leaching efficiencies. Similar behaviour of REs during leaching is evident from linear correlations between leaching efficiencies of La-Ce and Nd-Ce with a slope of unity in all three acids. However, in the case of phosphoric acid, a slope of 1.8 for La-Ce and 0.9 for Nd-Ce is a result of

the involvement of complexation and/or precipitation with phosphate ion and warrants further studies. The highest leaching efficiencies in H_3PO_4 (59% La > 38% Ce and 26% Nd) were observed after 10 min, but the precipitation of REs during prolonged leaching in all acids indicates the possibility of selective leaching of FAP which also warrants further studies with RE rich phosphate concentrates.

5. References

Al-Othman, A.O., Sweileh, J.A., 2000. Phosphate rock treatment with citric acid for the rapid potentiometric determination of fluoride with ion-selective electrode. Talanta 51, 993-999.

Antar, K., Jemal, M., 2008. Kinetics and thermodynamics of the attack of a phosphate ore by acid solutions at different temperatures. Thermochimica Acta 474, 32-35.

Bauer, D., Diamond, D., Li, J., Sandalow, D., Telleen, P., Wanneret, B., 2010. Critical Materials Strategy: US Department of Energy.

Brahim, K., Antar, K., Khattech, I., Jernal, M., 2008. Effect of temperature on the attack of fluorapatite by a phosphoric acid solution. Scientific Research and Essay Vol. 3(1), pp. 35-39.

Chaïrat, C., Schott, J., Oelkers, E.H., Lartigue, J-E., Harouiya, N., 2007. Kinetics and mechanism of natural fluorapatite dissolution at 25 ^{0}C and pH from 3 to 12. Geochimica et Cosmochimica Acta 71, 5901-5912.

Chakhmouradian, A.R., Reguir, E.P., Mitchell, R.H., 2002. Strontium-apatite: new occurrences, and the extent of Sr-for-Ca substitution in apatite-group minerals. The Canadian Mineralogist 40, 121-136.

Fernandes, A., Afonso, J.C., Dutra, A.J.B., 2013. Separation of nickel(II), cobalt(II) and lanthanides from spent Ni-MH batteries by hydrochloric acid leaching, solvent extraction and precipitation. Hydrometallurgy 133, 37-43.

Fleet, E.M., Pan, Y., 1995. Site preference of rare earth elements in fluorapatite. American Mineralogist, 80, 329-335.

Gupta, C.K., Krishnamurthy, N., 2005. Extractive Metallurgy of Rare Earths, first edition. CRC Press, Boca Raton, Florida.

Harouriya, N., Chaïrat, C., Köhler, S.J., Gout, R., Oelkers, E.H., 2007. The dissolution kinetics and apparent solubility of natural apatite in closed reactors at temperatures from 5 to 50 ^{0}C and pH from 1 to 6. Chemical Geology 244, 554-568.

Hunt, S., Senanayake, G., Stone, K., Perera, N., 2012. Calcium Phosphate Precipitation from Rare Earth Leach Liquors: Laboratory Test Work Program - Internal Report, Murdoch University (unpublished), pp1-77.

Industrial Minerals Company of Australia Pty Ltd (IMCOA), 2013. “Can China’s rare earths dynasty survive ?” extract. China’s Industrial Minerals and Markets Conference.

Johnson, R.H., Everett, L.S., David, C.S., 1995. Rare earth elements in hydrothermal systems: Estimates of standard partial molal thermodynamic properties of aqueous complexes of the

rare earth elements at high pressures and temperatures. Geochimica et Cosmochimica Acta 59. No. 21, 4329-4350.

Jordens, A., Cheng, Y.P., Waters, K.E., 2013. A review of the beneficiation of rare earth element bearing minerals. Minerals Engineering 41, 97-114.

Kim, C-J., Yoon, H-S, Chung, K,W., Lee, J-Y., Kim, S-D., Shin, S-M., Lee, S-J., Joe, A-R., Lee, S-Il., Yoo, S-J., Kim, S-H., 2014. Leaching kinetics of lanthanum in sulphuric acid from rare earth elements (REE) slag. Hydrometallurgy 146, 133-137.

Kim, E., Osseo-Asare, K., 2012. Aqueous stability of thorium and rare earth metals in monazite hydrometallurgy: Eh-pH diagrams for the systems Th-, Ce-, La-, Nd- (PO_4)-(SO_4)-H_2O at 25^oC. Hydrometallurgy 113-114, 67-78.

Kul, M., Topkaya, Y., Karakaya, I., 2008. Rare earth double sulfates from pre-concentrated bastnasite. Hydrometallurgy 93, 129-135.

Kuzmin, V.I., Pashkov, G.L., Lomaev, V.G., Voskresenskaya, E.N., Kuzmina, V.N., 2012. Combined approaches for comprehensive processing of rare earth metal ores. Hydrometallurgy 129-130, 1-6.

Levenspiel, O., 1972. Chemical Reactions Engineering. Wiley, New York.

Li, L., Xu, S., Ju, Z., Wu, F., 2009. Recovery of Ni, Co and rare earths from spent Ni-metal hydride batteries and preparation of spherical $Ni(OH)_2$. Hydrometallurgy 100, 41-46.

Lister, T.E., Wang, P., Anderko, A., 2014. Recovery of critical and value metals from mobile electronics enabled by electrochemical processing. Hydrometallurgy 149, 228-237.

Liu, X., Byrne, R.H., 1997. Rare earth and yttrium phosphate solubilities in aqueous solution. Geochimica et Cosmochimica Acta 61. No 8, 1625-1633.

Lokshin, E. P., Tareeva, O. A., Ivlev, K. G., Kashulina, T. G., 2007. Solubility of double alkali metal (Na, K) rare-earth (La, Ce) sulphates in sulphuric-phosphoric acid solutions at 20^{o}C.Russian Journal of Applied Chemistry 78. No. 7, 1058-1063.

Majima, H., Awakura, Y., 1981. Measurement of the activity of electrolytes and the application of activity to hydrometallurgical studies. Metall. Trans. 12B, 141-147.

McClellan, G.H., Lehr, J.R., 1969. Crystal chemical investigation of natural apatites. The American Mineralogist 54, 1374-1391.

Mendham, J., Denney, R.C., Barnes, J.D., Thomas, M.J.K., 2007. Vogel's quantitative chemical analysis, 5th ed., Pearson Education limited.

Moldoveanu, G,A., Papangelakis, V.G., 2012. Recovery of rare earth elements adsorbed on clay minerals: I. Desorption mechanism. Hydrometallurgy 117-118, 71-78.

Moldoveanu, G,A., Papangelakis, V.G., 2013. Recovery of rare earth elements adsorbed on clay minerals: II. Leaching with ammonium sulfate. Hydrometallurgy 131-132, 158-166.

Nakamoto, K., 2009. Infrared and Raman spectra of inorganic and coordination compounds: part A: Theory and applications in inorganic chemistry, 6th ed. A John Wiley & Sons inc. Publication.

Olanipekun, E., 1999. Kinetics of Dissolution of Phosphorite in Acid Mixtures. Bull. Chem. Soc Ethiop 13, 63- 70.

Panda, R., Kumari, A., Jha, M.K., Hait, J., Kumar, V., Kumar, J.R., Lee, J.Y., 2014. Leaching of rare earth metals (REMs) from Korean monazite concentrate. Journal of industrial and engineering chemistry 20, 2035-2042.

Preston, J., Cole, P., Craig, W., Feather, A., 1996. The recovery of rare earth oxides from phosphoric acid by-product, Part 1: Leaching of rare earth values and recovery of a mixed rare earth oxides by solvent extraction. Hydrometallurgy 41, 1-19.

Resende, L.V., Morais, C.A., 2010. Study the recovery of rare earth elements from computer scraps – Leaching experiments. Minerals Engineering 23, 277-280.

Roine, A., 2012. Outokumpu HSC Chemistry Thermochemical Database, Ver 7.1.

Outokumpu Research Oy, Finland.Sedlak, R.I., 1991. Phosphorus and nitrogen removal from municipal wastewater, 2nd ed. CRC press , 97-100.

Senanayake, G. Senaputra, A. Nicol, M. J., 2010. Effect of thiosulfate, sulfide, copper(II), cobalt(II)/(III) and iron oxides on the ammoniacal carbonate leaching of nickel and ferronickel in the Caron process. Hydrometallurgy 105, 60-68.

Senanayake, G., Jayasekera, S., Bandara, A. M. T. S., Koenigsberger, E., Koenigsberger, L., Kyle, J., 2014. Rare earth metal ion solubility in acidic sulphate-phosphate solutions. Proceedings of The 7th International Symposium - Hydrometallurgy 2014, Ed: E. Asselin, D. Dixon, F. Doyle, D. Dreisinger, M. Jeffrey, M. Moats, Canadian Institute of Mining, Metallurgy and Petroleum, Victoria, BC, Canada, Vol 1, pp. 313-324.

Senanayake,G., Kyle, J., Hunt, S., Stone, K., Perera, N., Jayasekera, S., 2014. Precipitation of calcium phosphate from hydrochloric acid leach liquor of a rare earth concentrate. Proceedings of The 7th International Symposium - Hydrometallurgy 2014, Ed: E. Asselin, D. Dixon, F. Doyle, D. Dreisinger, M. Jeffrey, M. Moats, Canadian Institute of Mining, Metallurgy and Petroleum, Victoria, BC, Canada, Vol 1, pp. 325-337.

Senanayake, G., 2007. Review of theory and practice of measuring proton activity and pH in concentrated chloride solutions and application to oxide leaching. Minerals Engineering 20, 634-645.

Senanayake, G., Muir, D.M., 2003. Chloride processing of metal sulphides: review of fundamentals and applications. Hydrometallurgy – 5th international conference, (Vol.1, pp. 517-531) Canada.

Sillen, L.G., Martell, A.E., 1964. Stability constants of metal complexes. Chemical Society Special Publication, Vol. 17. Chemical Society, London.

Sluis, S., Meszaros, Y., Marchee, W.J.M., Wesselingh, H.A., Rosmalean, G.M., 1987. The digestion of phosphate ore in phosphoric acid. Ind. Eng. Chem. Res, 26, 2501-2505.

Tunsu, C., Ekberg, C., Retegan, T., 2014. Characterization and leaching of real fluorescent lamp waste for the recovery of rare earth metals and mercury. Hydrometallurgy 144-145, 91-98.

Vijayalakshmi, R., Mishra, S.L., Singh, H., Gupta, C.K., 2001. Processing of xenotime concentrate by sulphuric acid digestion and selective thorium precipitation for separation of rare earths. Hydrometallurgy 61, 75-80.

Wang, L., Long, Z., Huang, X., Yu, Y., Cui, D., Zhang, G., 2010. Recovery of rare earths from wet-process phosphoric acid. Hydrometallurgy 101, 41- 47.

Williams, Q., Knittle, E., 1996. Infrared and Raman spectra of $Ca_5(PO_4)_3F_2$-fluorapatite at high pressures: compression-induced changes in phosphate site and Davydov splitting. J. Phys. Chem. Solids, 57. No. 4, 417-422.

Zhang, J., Edwards, C., 2012. A review of rare earth mineral processing technology. 44th Annual Canadian Mineral Processors Operators Conference, (pp. 79-102) Ottawa, Ontario.

Ziya, S.C., Scott, A.W., Christopher, H.G., 2005. The aqueous geochemistry of the rare earth elements: Part XIV: The solubility of rare earth element phosphates from 23 to 150 ^{0}C. Chemical Geology 217, 147– 169.

Zumdahl, S.S., Decoste, D.J., 2012. Chemical principles, 7th edition, Brooks Cole.

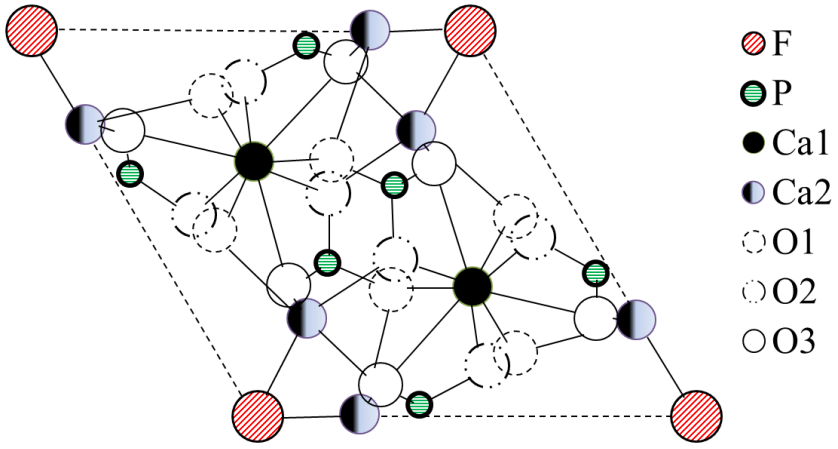

Fig. 1. Structure of FAP (reproduced from Fleet and Pan, 1995)

(a)

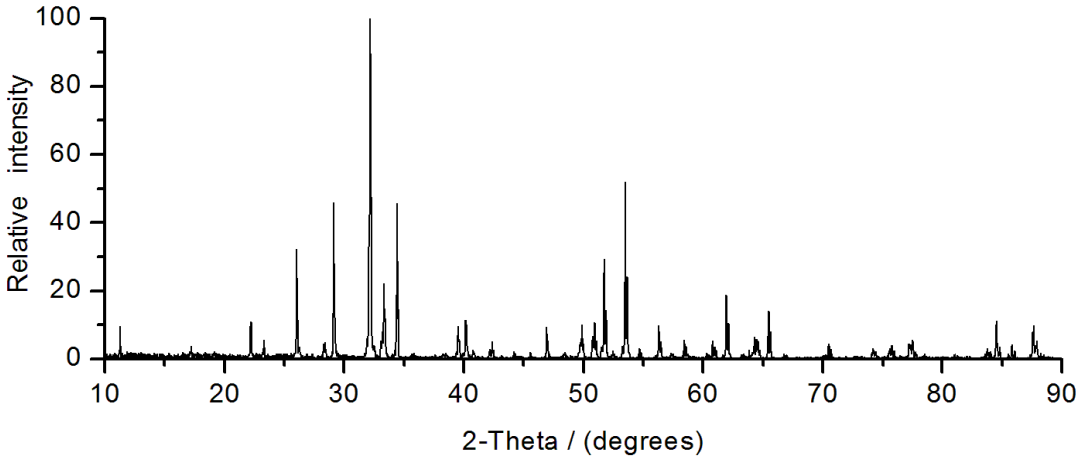

(b)

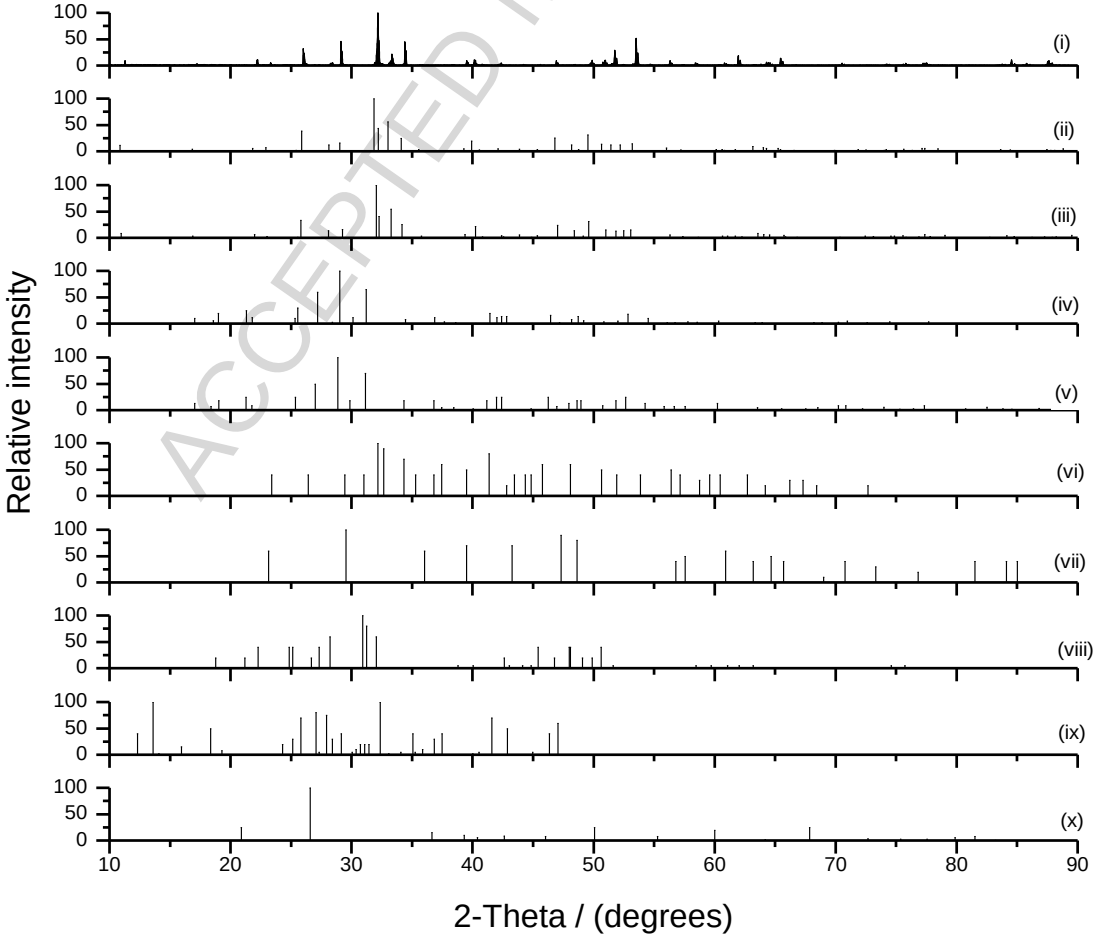

Fig. 2. (a) XRD analysis of feed material (FAP); (b) Comparison with standard patterns; (i) feed, (ii) FAP (01-071-5050), (iii) carbonate-FAP (01-073-9696), (iv) cheralite (00-033-1095), (v) monazite-Ce (00-011-0556), (vi) calcium silicate (00-002-0843), (vii) calcite (00-002-0623), (viii) britholite-La (00-013-0106), (ix) kainosite-Y (00-014-0332) and (x) silicon oxide (00-001-0649)

Figure 3

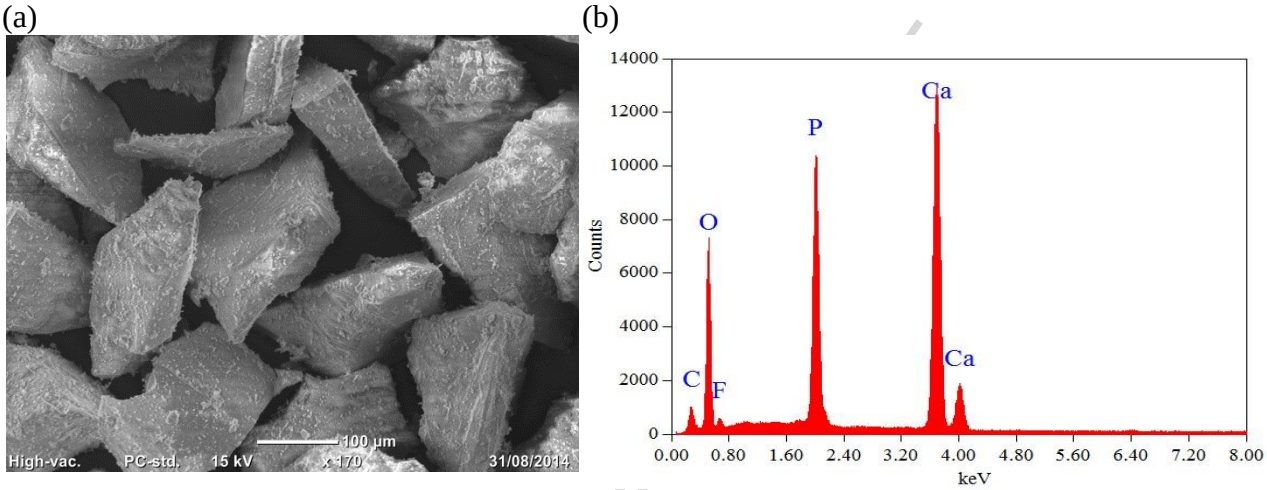

Fig. 3. (a) The SEM image and (b) EDS of FAP

Figures 4 and 5

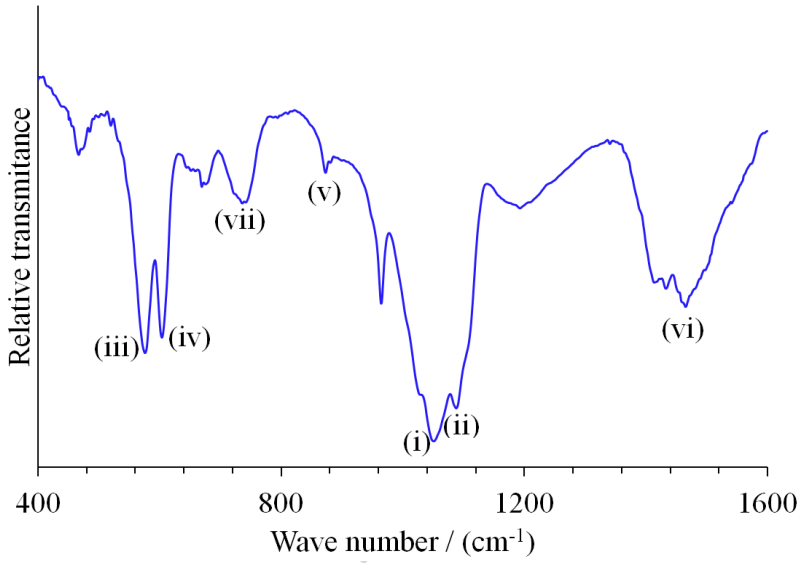

Fig. 4. The FT-IR spectrum of the FAP sample

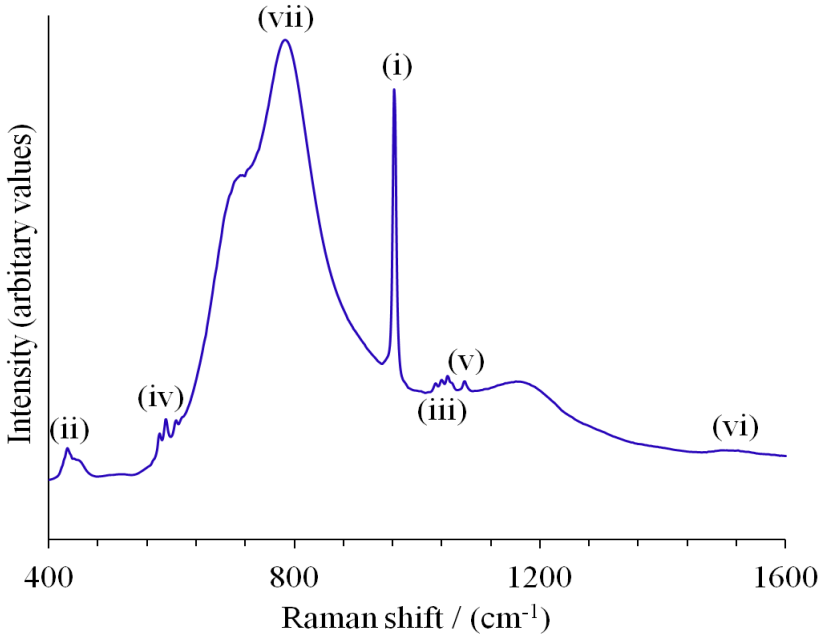

Fig. 5. The Raman spectrum of the FAP sample

Figure 6

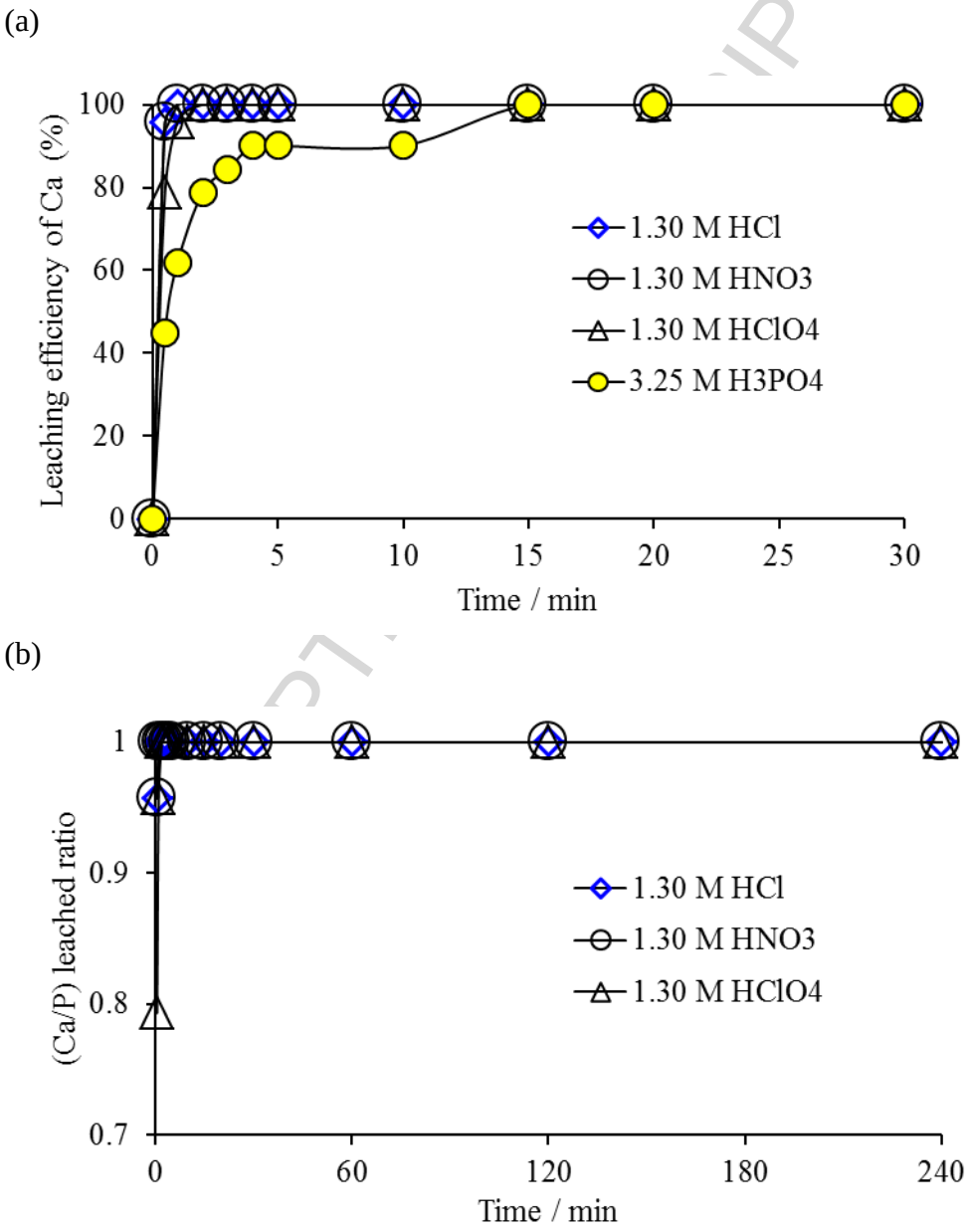

Fig. 6. The variation of % leaching of Ca from FAP : (a) Ca%, (b) leached Ca/P molar ratio

Figure 7

(a) (b)

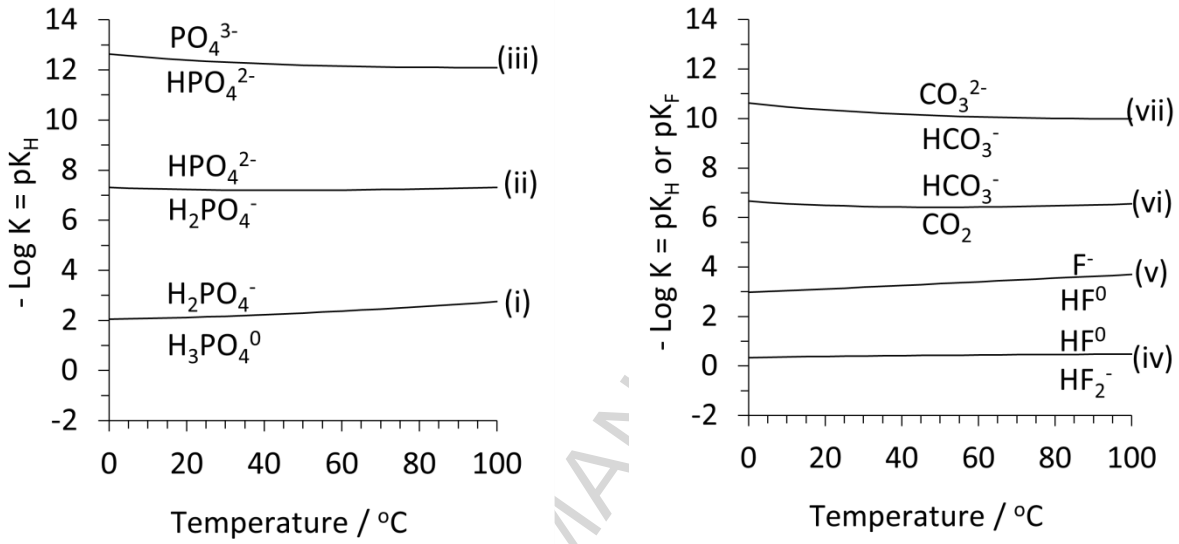

Fig. 7. Effect of temperature on acid dissociation equilibrium constants from HSC 7.1 database assuming equimolar concentrations of conjugate species HA and A^- in Eqs. (25)-(27) (Senanayake et al., 2014b)

Figure 8

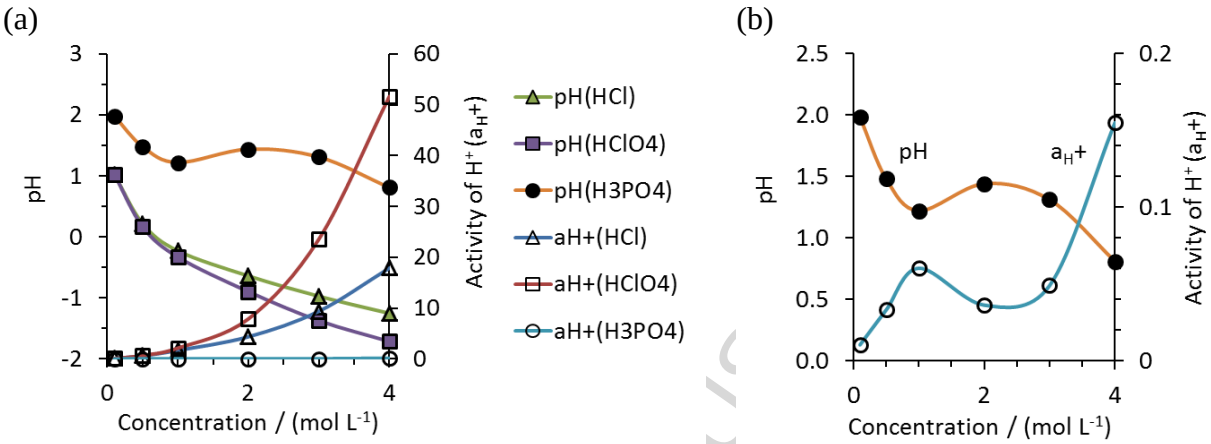

Fig. 8. Effect of acid concentration on proton activity and pH at 25°C (data from Majima and Awakura, 1981; Senanayake , 2007 (HCl and $HClO_4$, corrected for liquid junction potentials) and this work (H_3PO_4 , assuming negligible liquid junction potentials due to low dissociation of H_3PO_4).

Figure 9

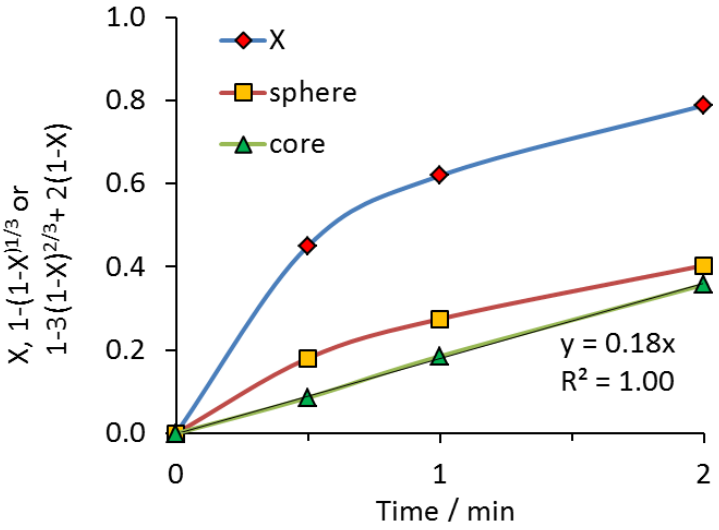

Fig. 9. Applicability of kinetic models for calcium leaching from FAP in 3.25 M H_3PO_4 (data from Fig. 6a).

Figure 10

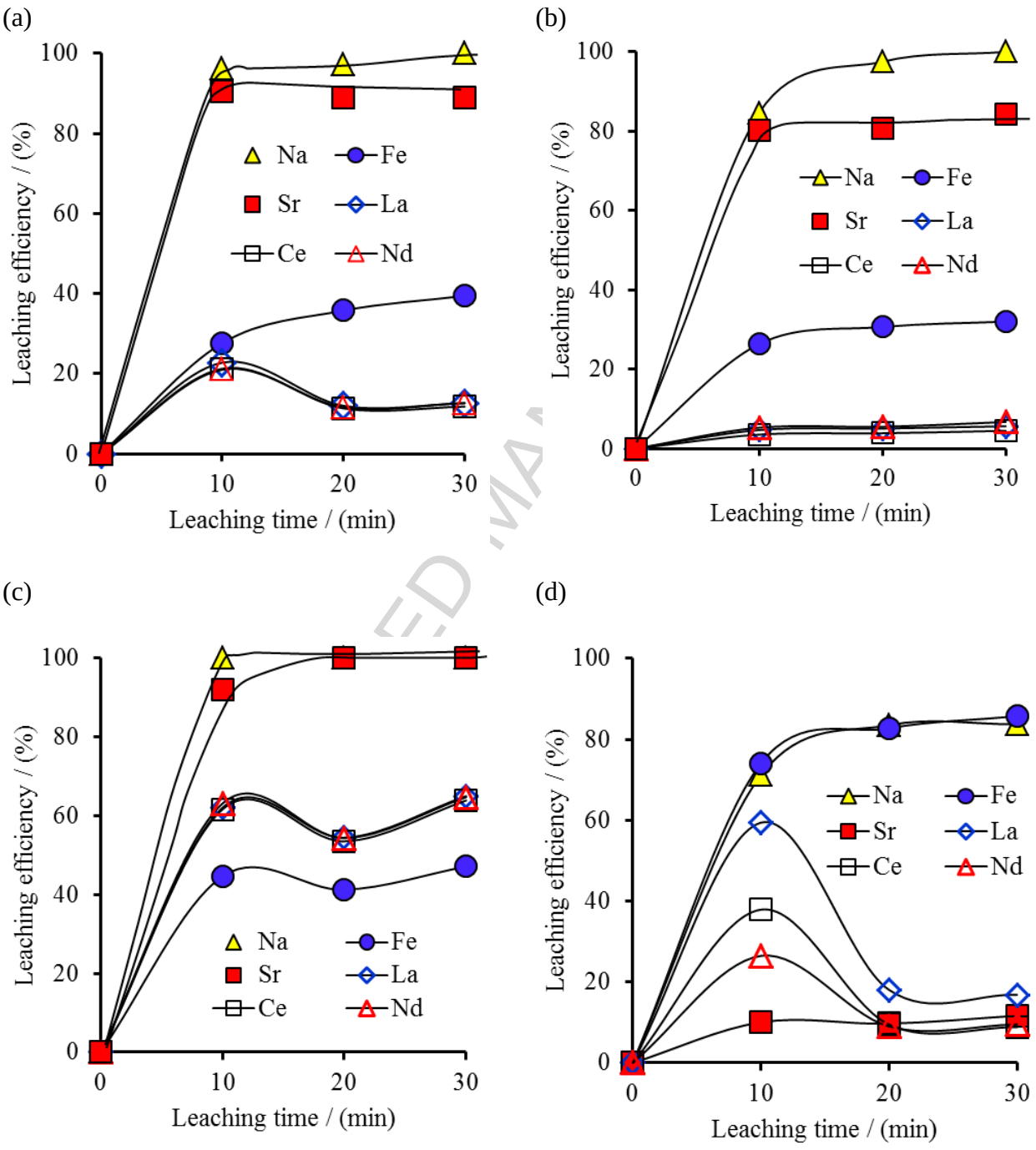

Fig. 10. Effect of 3.25 mol/L H_3PO_4 and 1.30 mol/L other acids on leaching efficiency (a) HCl, (b) HNO_3, (c) $HClO_4$ and (d) H_3PO_4

Figure 11

(a)

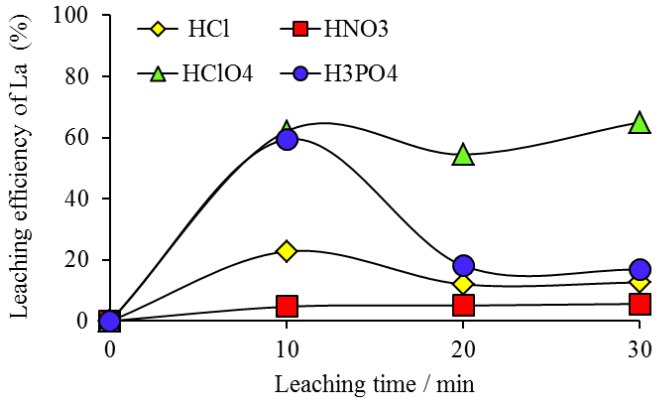

(b)

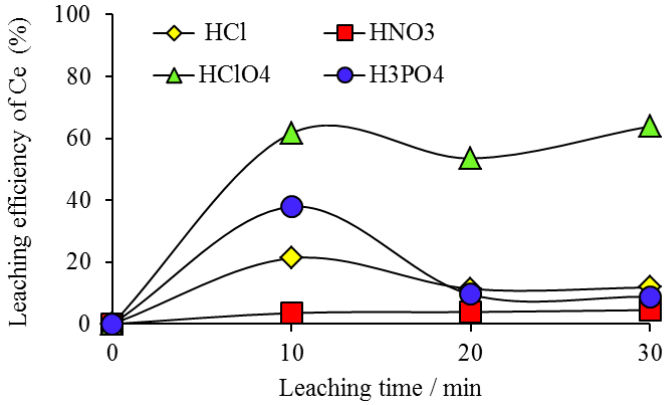

(c)

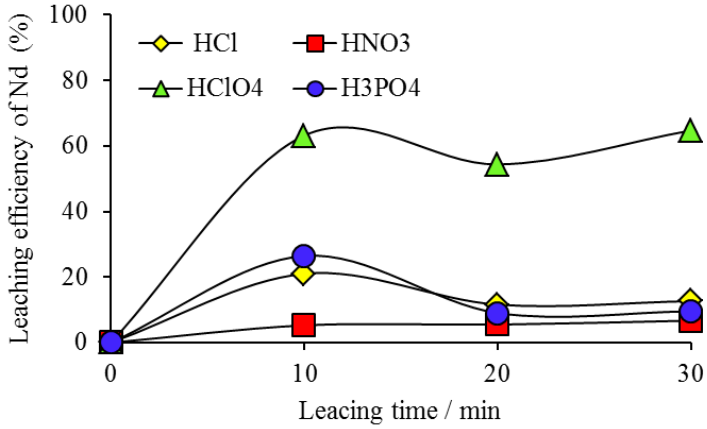

Fig. 11. Comparison of RE leaching efficiency in different acids as in Fig. 10: (a) La, (b) Ce, (c) Nd

Figure 12

(a)

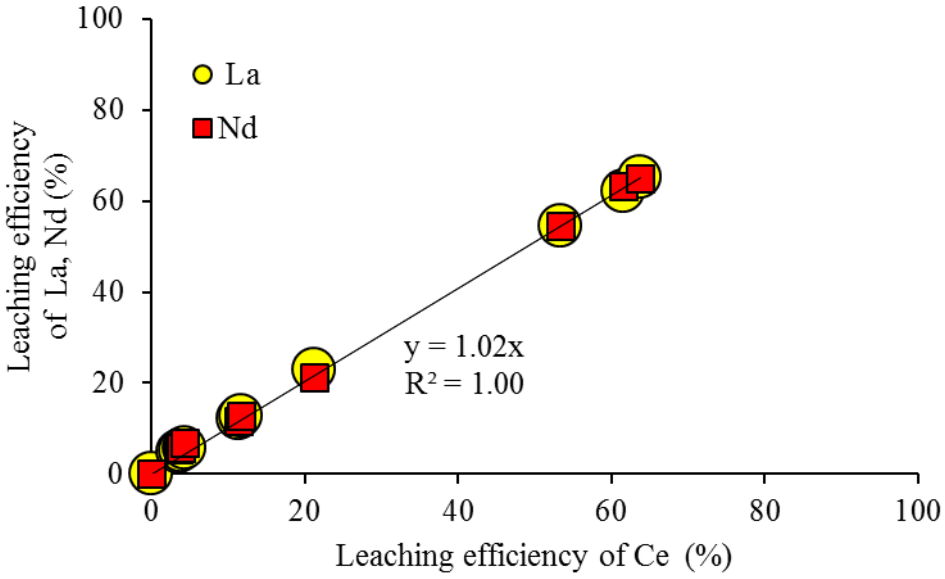

(b)

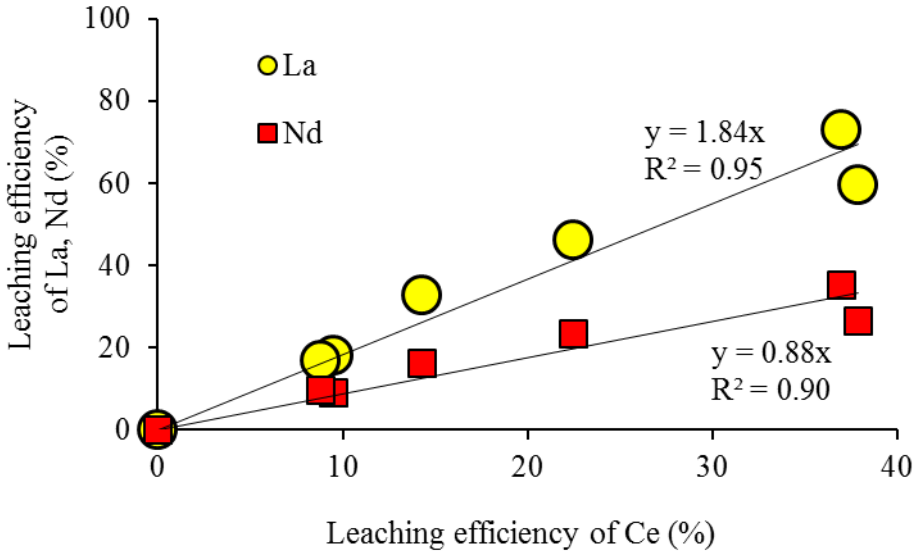

Fig. 12. Correlation between leaching efficiency of REs in (a) HCl, HNO_3 and $HClO_4$ and (b) H_3PO_4

Table 1. The world RE-oxide production and the reserves

Country	RE-oxide Production / (Mt)		Reserves* / (Mt)
	2012	2013	
China	100, 000	100,000	55,000,000
United States	800	4,000	13,000,000
India	2,900	2,900	3,100,000
Australia	3,200	2,000	2,100,000
Brazil	140	140	22,000,000
Malaysia	100	100	30,000
Other countries	2,620	2,620	41,000,000
Total (rounded)	110,000	110,000	140,000,000

Source: U.S. Geological Survey, Mineral Commodity Summaries, February 2014, * a working inventory of mining companies' supply of an economically extractable mineral commodity

Table 2. Types of RE minerals

Type	Mineral name	Chemical formula
Oxides	Aeschynite	$(Ce,Ca,Th)(Ti,Nb)_2O_6$
	Euxenite	$(Y,Ce,Ca,U,Th)(Ti,Nb,Ta)_2O_6$
	Fergusonite	$(Y,Sr,Ce,U)(Nb,Ta,Ti)O_4$
	Loparite	$(Na,Ca,Ce,Sr)_2(Ti,Ta,Nb)_2O_6$
	Priorite	$(Y,Er,Ca,Th)(Ti,Nb)_2O_6$
	Samarskite	$(Y,Er,U,Ce,Th)_4(Nb, Ta)_6O_2$
Carbonates	Ancylite	$Sr(Ce,La)(CO_3)_2(OH).H_2O$
	Bastnasite	$(Ce,La,Pr)(CO_3)F$
	Parisite	$Ca(Ce,La...)_2(CO_3)F_2$
	Synchisite	$Ca(Ce,Nd,Y,La)(CO_3)_2F$
	Tengerite	$Y_2(CO_3)_3.nH_2O$
Phosphates	Monazite	$(Ce,La,Th,Nd,Y)PO_4$
	Florencite	$(La,Ce)Al_3(PO_4)_2(OH)_6$
	Xenotime	YPO_4
	Cheralite	$(Ca,Ce)(Th,Ce)(PO_4)_2$
	Britholite	$(Na,Ce,Ca)_5(OH, F)((P,Si)O_4)_3$
Silicates	Thorite	$ThSiO_4$
	Orthite	$(Ca,Ce)_2(Al,Fe)_3Si_3O_{12}(O,OH)$
	Kainosite	$Ca_2(Ce,Y)_2(SiO_4)_3CO_3.H_2O$
	Thalenite	$Y_2(Si_2O_7)$

(Bauer et al., 2010; Gupta and Krishnamurthy, 2005)

Table 3. Previous studies on FAP leaching with different lixiviant systems

Feed material	Lixiviant	Conditions			References
		% (w/w)	Temp. / (^{o}C)	(S/L)*	
Synthetic FAP	H_3PO_4	24.8	25- 60	0.67	Brahim et al., 2008
Phosphate ore	(i) H_3PO_4 (ii) 4:1 (v/v) mixture of H_3PO_4 and H_2SO_4	(i) 27.6 (ii) 27.6 & 90	25 - 80	0.4 – 11.4	Antar and Jemal, 2008
Natural FAP	HCl, KH phthalate and NaOH (pH = 1-6)	NR	5 - 50	0.07 – 0.68	Harouiya et al., 2007
Natural FAP	HCl/NaCl, NH_3/NH_4Cl, NaOH/NaCl (pH = 3-12)	NR	25	0.15 – 3.25	Chaïrat et al., 2007
Phosphate rock[a]	Citric acid	0.2 – 38.4	22 - 80	0.05 – 1.00	Al-Othman and Sweileh, 2000
Phosphorite (phosphate rock)	H_2SO_4 and HCl mixture (i) H_2SO_4 (ii) HCl	(i) 0 - 53.9 (ii) 0 – 8.8	60 - 90	2.0	Olanipekun, 1999
Phosphate ore	H_3PO_4	41.4 – 69.0	60 - 90	2.0 – 8.0	Sluis et al., 1987

* Solid to liquid ratio as % (w/v), a = Laboratory test work with small quantities, NR = Not Reported

Table 4. Elemental assays of non-REs and REs in FAP

Non-RE	Na	Mg	Al	Si	P	F*	S	K	Ca	Fe	As	Se	Sr	Th	U
Mass %	0.19	0.01	0.00	0.09	12.6	2.10	0.00	0.09	33.8	0.22	<0.01	<0.01	0.32	0.01	<0.01

RE	Y	La	Ce	Pr	Nd	Sm	Eu	Gd	Tb	Dy	Ho	Er	Tm	Yb	Lu
Mass %	0.02	0.11	0.24	0.03	0.10	0.02	<0.01	0.02	<0.01	0.01	<0.01	<0.01	<0.01	<0.01	<0.01

*Fluoride assay based on XRF.

Table 5. Band assignment of FT-IR spectrum of FAP

Vibrational modes	Peak no:	IR frequency / (cm^{-1})				Assignment
		This work	Literature data			
		FAP	Nakamoto (2009)		Williams and Knittle (1996)	
			Inorganic Compounds	Calcite	FAP	
$\nu_3(f_2)$ / ν_d(P-O)	(i),(ii)	1051, 1088	1000 - 1080		1038, 1097	PO_4^{3-}
$\nu_4(f_2)$ / δ_d(O-P-O)	(iii),(iv)	575, 603	520 - 610		570, 600	
$\nu_2(a^{11}{}_2)$ / $\pi(CO_3)$	(v)	872	810 - 890	879		CO_3^{2-}
$\nu_3(e^1)$ / ν_d(C-O)	(vi)	1465	1420 - 1480	1429 - 1492		
$\nu_4(e^1)$ / δ_d(O-C-O)	(vii)	735	680 - 750	706		

Peak numbers are as shown in Fig. 4. Abbreviations used in modes are ν: stretching, δ: in-plane bending or deformation, s: symmetric, as: asymmetric and d: degenerate

Table 6. Band assignment of Raman spectrum of FAP

Vibrational modes	Peak no:	Raman shift / (cm^{-1})				Assignment
		This work	Literature data			
			Nakamoto (2009)		Williams and Knittle (1996)	
		FAP	Inorganic compounds	Calcite	FAP	
$\nu_1(a_1)$ / ν_s(P-O)	(i)	963	960		968	PO_4^{3-}
ν_2(e) / δ_d(O-P-O)	(ii)	430	450		447	
$\nu_3(f_2)$ / ν_d(P-O)	(iii)	1050	1000 - 1080		1034, 1061	
$\nu_4(f_2)$ / δ_d(O-P-O)	(iv)	590,607	520 - 610		580, 611	
$\nu_1(a^1{}_1)$ / ν_s(C-O)	(v)	1077	1020 - 1090	1087		CO_3^{2-}
$\nu_3(e^1)$ / ν_d(C-O)	(vi)	1495	1420 - 1480	1432		
$\nu_4(e^1)$ / δ_d(O-C-O)	(vii)	785	680 - 750	714		

Peak numbers are as shown in Fig. 5. Abbreviations used in vibrational modes are same as in Table 5

Table 7. Leaching efficiencies of metal ions and phosphate from FAP in different acids

Acid	Concentration (mol/L)	Leaching time (min)	Leaching efficiency (%)								
			Ca	P	Na	Fe	Sr	La	Ce	Nd	F
HCl	1.30	10	100	100	96.3	27.6	90.5	22.8	21.3	21.0	
		20	100	100	97.2	35.8	88.9	12.0	11.4	11.6	
		30	100	100	100	39.5	88.9	12.6	11.8	12.7	
	3.25	30	100	100							100
HNO_3	1.30	10	100	100	84.6	26.3	80.2	4.68	3.52	5.28	
		20	100	100	97.5	30.7	80.7	5.06	3.86	5.51	
		30	100	100	100	32.0	84.2	5.62	4.49	6.71	
	3.25	30	100	100							100
$HClO_4$	1.30	10	100	100	100	44.7	92.0	62.1	61.7	63.2	
		20	100	100	100	41.2	100	54.5	53.5	54.4	
		30	100	100	100	47.1	100	65.0	63.9	64.8	
	3.25	30	100	100							92.2
H_3PO_4	2.28	30	75.0								100
	3.25	10	90.1	_	71.1	74.0	10.1	59.4	37.9	26.5	
		20	100	_	83.5	82.7	9.7	18.1	9.5	9.0	
		30	100	_	83.7	85.7	11.7	16.8	8.8	9.5	100
		60	100	_	95.3	93.3	12.9	72.8	37.0	35.3	
		120	100	_	100	87.5	13.1	46.1	22.5	23.5	
		240	100	_	100	100	13.4	32.7	14.3	16.2	

Temperature = 95 ^{o}C; Acid concentrations: HCl, HNO_3 and $HClO_4$ = 1.30 mol/L and 3.25 mol/L (1.25 and 3.12 times the stoichiometric amounts respectively based on Eqs. 1-3), H_3PO_4 = 2.28 mol/L and 3.25 mol/L (3.12 and 4.45 times the stoichiometric amounts respectively based on Eq. 4)

Table 8.Equlibrium constants of some reactions

Reaction	Eq.	pKa or pK_H	Log K	-log K_{sp} (pK_{sp})
$H_3PO_4 + H_2O = H_2PO_4^- + H_3O^+$	(6)	2.15[a]		
$H_2PO_4^- + H_2O = HPO_4^{2-} + H_3O^+$	(7)	7.21[a]		
$HPO_4^{2-} + H_2O = PO_4^{3-} + H_3O^+$	(8)	12.3[a]		
$HF_2^- = HF + F^-$	(9)	0.7[b] (pK_F)		
$HF = H^+ + F^-$	(10)	2.91[b]		
$CO_{2(aq)} + H_2O = H^+ + HCO_3^-$	(11)	6.37[a]		
$HCO_3^- = H^+ + CO_3^{2-}$	(12)	10.3[a]		
$Ca^{2+} + HPO_4^{2-} = CaHPO_4^0$	(13)		2.80[c]	
$Ca^{2+} + HPO_4^{2-} + H^+ = Ca(H_2PO_4)^+$	(14)		8.30[c]	
$Fe^{3+} + H_2PO_4^- = Fe(H_2PO_4)^{2+}$	(15)		21.8[d]	
$10Ca^{2+} + 6PO_4^{3-} + 2F^- = Ca_{10}(PO_4)_6F_2$	(16)			118[e]
$3Ca^{2+} + 2PO_4^{3-} = Ca_3(PO_4)_2$	(17)			31.9[f] ,30.7[g]
$3Sr^{2+} + 2PO_4^{3-} = Sr_3(PO_4)_2$	(18)			31.0[f]
$Fe^{3+} + PO_4^{3-} = FePO_4$	(19)			24.4[g]
$Ca^{2+} + F^- = CaF^+$	(20)		0.59[b]	
$Fe^{2+} + F^- = FeF^+$	(21)		0.83[b]	
$Fe^{3+} + F^- = FeF^{2+}$	(22)		5.41[b]	
$Fe^{3+} + 2F^- = FeF_2^+$	(23)		9.85[b]	
$Fe^{3+} + 3F^- = FeF_3^0$	(24)		12.3[b]	

At 25 ^oC and ionic strength 0-1

a. Mendham et al. (2007)

b. Hunt et al. (2012) and Sillen and Martell (1964)

c. Lokshin et al. (2007)

d. Sedlak (1991)

e. Chaİrat et al. (2007)

f. Zumdahl and Decoste (2012)

g. HSC7.1 database

Table 9. Formation constants and solubility products for rare earth phosphate complexes and solids

RE^{3+}	Formation Constants (log K)			-log K_{sp} (pK_{sp}) $RE.PO_4$ (solids)
	$RE(HPO_4)^{+}$	$RE(H_2PO_4)^{2+}$	$RE(HPO_4)_2^{-}$	
La^{3+}	4.10	2.50		26.2 (26.4[b])
Ce^{3+}	4.32	2.43		
Nd^{3+}	4.54(4.69[a])	2.31	7.68[a]	25.9 (26.2[b])

(a) Kim and Osseo-Asare (2012), (b) Liu and Byrne (1997), Johnson et al. (1995); Ziya et al. (2005).

Highlights

- High proton activity and anion participation facilitate cation leaching
- Interaction with chloride and phosphate affects calcium and RE leaching
- RE leaching efficiency in acids: $HClO_4 > H_3PO_4 > HCl > HNO_3$
- La-Ce and Nd-Ce leaching efficiency correlations have a slope ≈ 1
- Precipitation of RE in phosphoric acid during prolonged leaching facilitate selective leaching of calcium and minor metal ions